Egypt. J. Chem. **Vol. 65**, No. 6 pp. 647 - 664 (2022)

Egyptian Journal of Chemistry

http://ejchem.journals.ekb.eg/

Synthesis and Characterization of Binary Chelates Derived from *1*-Hydroxy-*2*-Naphthoic (L^1) and *2*-Hydroxy-*1*-Naphthoic (L^2) Acids with Some Metal Ions by Tribochemical Reactions and Its Application as Anticancer

Aml G. Ahmed[1], Eman M. Shoukry[1*] and Mohsen M. Mostafa[2]

[1]*Faculty of Science (Girl branch), Al-Azhar University, Egypt*

[2]*Faculty of Science, Mansoura University, Egypt*

**Corresponding author. E-mail address:* eman_shoukry2002@azhar.edu.eg

Abstract

New binary chelates derived from ligands ($\mathbf{L^1}$ and $\mathbf{L^2}$) were synthesized by tribochemical reaction in the solid state. The isolated chelates are characterized by chemical, spectral (IR, UV-Visible, ^{1}H-NMR, mass) and magnetic methods. IR data suggest that the ligands ($\mathbf{L^1}$and $\mathbf{L^2}$) behave in a bidentate manner***via*** the phenolic OH and the CO (carboxylate) groups without displacement of a hydrogen atom from the carboxylate and/or the phenolic groups. The geometries of the isolated solid complexes were illustrated by spectral and magnetic data and confirmed by material studio program.DFT calculations suggest the most suitable geometry as well as the stability of the complexes. The bond lengths, bond angles, chemical reactivity, binding energies and dipole moments for all compounds were evaluated using density functional theory and molecular electrostatic potential for $\mathbf{L^1}$and $\mathbf{L^1}$. The mass spectra of some metal chelates illustrate that these compounds are existed as dimer. Some chelates were tested against fungi and bacteria. Also, the ligands and some of their complexes were tested as anticancer using **MCF-7** cells (human breast cancer cell line) and **HepG-2** cells (human Hepatocellular carcinoma).

Keywords:*1*-Hydroxy-*2*-naphthoic acid ($\mathbf{L^1}$)*,2*-hydroxy-*1*-naphthoic ($\mathbf{L^2}$) acid, binary complexes, tribochemical reaction, green chemistry, biological activity

1. Introduction

There is a growing interest in studying the synthesis of chelates using tribochemical reactions as well as the characterization of the isolated compounds using the various methods including chemical, spectral (IR, UV-Vis., ^{1}H-NMR and mass) and magnetic measurements. Also, tribochemical as a type of green chemistry is considered as a marvelous method for synthesis of solid complexes in absence of solvent. Also, this study is used to explain the behavior of proteins and enzymes in organisms during the synthesis of proteins. Amino acids are considered as good example to get a better insight into the characteristics of naturally occurring copper metallo-proteins **[1]**.Several Cu^{2+} chelates involving simple ligands have displayed diverse pharmacological activities i.e., copper complexes

DOI: 10.21608/EJCHEM.2021.106188.4883

exhibit anti-inflammatory and cytostatic activities **[2,3].**Hydroxynaphthoic acids are important chemicals that find use in numerous applications including pharmaceuticals and medical**[4,5].**Also, in continuation of our earlier work **[6-14]** on the synthesis of metal complexes by tribochemical reactions as an example of green chemistry **[15,16],**we embarking on this technique to synthesis and characterizing of new binary metal complexes. These chelates were derived from different metal ions (Cu^{2+}, Co^{2+}, Ni^{2+}, Mn^{2+}, Cd^{2+}, Hg^{2+}, Cr^{3+}) with *1*-hydroxy-*2*-naphthoic (**L^1**) and *2*-hydroxy-*1*-naphthoic (**L^2**)acids. The detached complexes were distinctive using different chemical, physical, spectral, magnetic measurements. Material studio program was used for calculating HUMO, LUMO, and DFT parameters on the atoms to confirm the geometry of the isolated compounds. In continuation of our earlier work as well as the work done by another coworker**[17-18]** concerning synthesis of binary complexes using tribochemical reactions, we embarked on this type of reaction to investigate the binary complexes to study the biological significance **[19-21]**. Biological activity of **L^1, L^2** and some metal complexes of **L^1**was examined.

2. Experimental

2.1. *Materials*

1-Hydroxy-*2*-naphthoic (**L^1**) and *2*-hydroxy-*1*-naphthoic acids (**L^2**) were obtained from Aldrich. The metal chlorides (Cu^{2+}, Co^{2+}, Ni^{2+}, Mn^{2+}, Cd^{2+}, Hg^{2+} and Cr^{3+}) used in the synthesis of the solid metal chelates were of AR quality. The solid complexes of the binary chelates were synthesized by tribochemical reactions and in absence of solvent.

2.2.*Instrumentation*

Carbon and hydrogen contents were carried out at the Microanalytical Unit at Cairo University, Egypt. Copper and chloride contents of the chelates have been determined by volumetric and gravimetric methods **[22].**IR spectra (4000–400 cm^{-1}) as KBr discs and/or nujol mull were recorded on a Mattson 5000 FTIR spectrophotometer. Electronic spectra were recorded on an ATI Unicom UV-Vis spectrophotometer version software V3-20. Magnetic measurements were carried out at room temperature (298 K) on a Sherwood magnetic balance. ^{1}H-NMR spectra in d_6-DMSO were carried out in the micro analytical center at Cairo University. The mass spectra of chelates were carried out using Hewlett-Packard instrument model MS-5988 GS/MS at 70 eV. ***In vitro*** cytotoxicity tests were conducted utilizing some metal chelates against MCF-7, HepG-2 and HCT-116 cell lines using a colorimetric assay (MTT assay) at the Regional Center for Mycology and Biotechnology, Al-Azhar University, Egypt. Also the ligands and its chelates were tested as antimicrobial (Gram +ive and Gram –ive), antifungal (Aspergillus flavus and Candida albians) and anticancer on **MCF-7** cells (human breast cancer cell line), and **HepG-2** cells (human Hepatocellular carcinoma).

2.3. *Synthesis of binary chelates derived from L^1 and L^2 using tribochemical reaction*

The metal binary chelatesderived from **L^1** and **L^2** with some metal chloride **(**Cu^{2+}, Co^{2+}, Ni^{2+}, Mn^{2+}, Cr^{3+}, Cd^{2+} and Hg^{2+}) were prepared by grinding equivalent amounts of **L^1** and/or **L^2** with the above mentioned metal chlorides in agate mortar for 1 h. The grinding process was continued till the reactants became very find powder. The products were dried in an oven for 1 h at 60 °C. After that the products were grinded well again in a mortar for 30 minutes and finally kept in a desiccator over anhydrous $CaCl_2$. The results of elemental analyses with some physical data are recorded in **Table 1.**

2.4. *Biological studies*

2.4.1. *Cytotoxicity evaluation using viability assay*

The effects of **L^1, L^2** and some metal complexes of **L^1**on **MCF-7** cells (human breast cancer cell line) and **HepG-2** cells (human Hepatocellular carcinoma)of epitheliod carcinoma cervix cancer (Hela) were recorded by colorimetric assay where the colorimetric test is measured and recorded at absorbance of 490 nm utilizing a plate reader (EXL 800). The relative cell practically in rate was computed as (A570 of treated examples/A570 of untreated specimen) x 100**[23,24]**and the effect on mammary gland breast cancer (MCF-7) observed with ELISA **[23-25]**and the percentage of viability was calculated as [1-(ODT/ODC)] x 100 % where ODT is the mean optical density of wells treated with the tested compounds and ODC is the mean optical density of untreated cells.

2.4.2.Antibacterial and antifungal activity

The disc diffusion method **[26-27]**was the method that used in testing two crystal compounds against two antibacterial of the types (Gram-positive, *Staphylococcus aurous*), Gram-negative, *Escherichia coli*) and two Antifungal of the types (Candida *albicans* and Aspergillum flavus). The activity index was calculated by the following formula,

% Activity Index = [Zone of inhibition by test compound (diameter) x100] / **[**Zone of inhibition by standard (diameter)**]**

3. Results and Discussion

The chemical analyses with some physical properties of the binary chelates are listed in **Table 1**. The results indicate that the melting points of the chelates lie in the range 102-250 ^oC suggesting that the bond between the ligand and the metal ions is quite weak. Also, the low melting point is explained on the basis of the simple coordination of the ligand to the metal salts. The complexes are quite stable against air and light for more than one year. All the complexes are soluble in ethanol and dimethyl sulphoxide and insoluble in all non-polar solvents. The values of molar conductance in DMSO for the complexes lie in the range 2.0-9.0 ohm^{-1}. cm^2. mol^{-1} suggest that these complexes are nonelectrolyte in nature. The insolubility of the complexes in most organic solvents except DMSO is taken as additional evidence for the nonelectrolyte nature of the compounds. The structures of **L^1 and L^2** are represented as shown in**Figs. 1 and 2**, respectively. Fourteen complexes (**1-14**) separated from **L^1 and L^2** are set out in **Table 1**

3.1. IR spectra

The IR spectra of the freeligands **(L^1**and **L^2)** in KBr show two splitting bands for each ligand at 3055, 2993; 2843 and 2808 $cm^{-1}$for **L^1** while at 3060, 3003; 2855 and 2813 cm^{-1} for **L^2,** respectively. The four bands are assigned to the free OH(phenolic), free OH(COOH), hydrogen-bonded OH(phenolic) and hydrogen-bonded OH(COOH), respectively. The observation of four bands for both **L^1** and **L^2** supports that each ligand contains equilibrium mixture of the free and hydrogen-bonded OH (inter- and/or intra-hydrogen bonded). The observation of these bands at lower wavenumber is mainly due to the existence of a strong hydrogen bonding for the carboxylic and OH groups. Moreover, the observation of weak and broad bands in the 1800-2200 cm^{-1} region supports the presence of strong hydrogen of the type O-H…..O **(Fig. 3) [28].**Finally, the observation of a strong band at 1643 for **L^1** and at 1636 cm^{-1} for **L^2** isattributed to the ν(C=O) vibration. Theexistence of this band at lower wavenumberconfirmsthat this band is existed under the influence of strong hydrogen bonding as discussed before.

On comparing the IR spectra of the ligands (**L^1**and**L^2)** with its chelates we observed negative shifts of both the carbonyl and OH(phenolic) groups to lower

wavenumbers indicating the participation of these groups in bonding. Finally, the observation of two new bands in the 535-532 and 475-470 cm^{-1} regions for ligand $\mathbf{L^1}$ are assigned to ν(M-O) for OH phenolic and ν(M-O) for the carbonyl of the COOH groups**[29]**, respectively. Also, the observation of two new bands in the 540-535 and 463-458 cm^{-1} region for ligand $\mathbf{L^2}$ are assigned to ν(M-O) for OH phenolic and ν(M-O) for the carbonyl of the COOH groups, respectively. All these observations suggest the participation of these groups, carbonyl oxygen and the hydroxyl groups of the phenol groups, in coordination.

3.2. ^{1}H-NMR spectra

The ^{1}H-NMR spectra of $\mathbf{L^1}$ and $\mathbf{L^2}$ in d_6-DMSO shows two signals at12.2 and 9.7 ppm assigned to the protons of the OH(COOH) and OH of the (phenolic) groups for $\mathbf{L^1}$ while at 11.9 and 9.6 ppm for $\mathbf{L^2}$, respectively. The observation of the former signal downfield of TMS suggests that the OH(COOH) contains a strong hydrogen bonding in comparison to the second signal. Both signals are disappeared on adding D_2O. The multiple signals in 7.1-8.4 ppm region are attributed to the protons of the naphthoic moiety. The ^{1}H-NMR spectra of the Hg(II) and Cd(II) complexes derived from $\mathbf{L^2}$, [Hg$\mathbf{L^2}$$Cl_2$].$2H_2O$ **(Fig. 4)** and[Cd$\mathbf{L^2}_2Cl_2$].$3H_2O$ **(Fig. 5),**show two signals for each at 12.7, 6.6; 12.55 and 6.7 ppm attributed to the protons of the OH ((COOH)) and OH(phenolic) groups, respectively. The shift of the latter signal in comparison to that observed in case of the free ligand is taken as evidence for the participation of both the OH and the carbonyl of the carboxylate in coordination. A broad signal at 3.6 ppm is observed in the spectra of both complexes is assigned to the protons of hydrated H_2O which disappear on adding D_2O **(Figs. 6, 7)**.

3.3. Mass spectra

The mass spectra of three complexes with the general formulae, [Mn($\mathbf{L^1}_2$)Cl_2].$4H_2O$, [Mn($\mathbf{L^2}_2$)Cl_2].$10H_2O$ and [Co(L_2)$_2$)Cl_2].$3H_2O$ were carried out. The spectra suggest that these chelates are mainly existed as a dimer. The mass spectrum of [Mn($\mathbf{L^1}_2$)Cl_2].$4H_2O$ is represented in **Fig. 8.**

3.4. Electronic spectra and magnetic moments

The electronic spectra of the metal chelates (Cu^{2+}, Co^{2+}, Ni^{2+}, Mn^{2+}, Cr^{3+}) in DMSO suggest that all the isolated binary chelates have octahedral geometry around the metal ions. The electronic spectra of the two pink Co(II) complexes, [Co$\mathbf{L^1}$$Cl_2$($H_2O$)$_2$] (**4**) and [Co$L^2{}_2Cl_2$]$_2$.$3H_2O$ (**9**), in DMSO shows three bands for each chelate. The first one (**4**) shows three bands at 20833, 19833 and 15625 cm^{-1} in DMSO assigned to $^4T_{1g} \rightarrow {}^4T_{2g}$ *(F),*$^4T_{1g} \rightarrow {}^4T_{2g}$ *(P)* and $^4T_{1g} \rightarrow {}^4A_{2g}$ transitions, respectively. Also, the second Co(II) complex (**9**) exhibits three bands in DMSO at 20921, 19608 and 15873 cm^{-1} attributed to $^4T_{1g} \rightarrow {}^4T_{2g}$ *(F),* $^4T_{1g} \rightarrow {}^4T_{2g}$ *(P)* and $^4T_{1g} \rightarrow {}^4A_{2g}$ transitions in an octahedral geometry around the Co(II) ions [**30**]. Also, the values of magnetic moments for the two complexes (**4** and **9**) are 5.47 and 5.10 BM, respectively, in accordance with the values reported in literature **[31]**. Moreover, the values of **ε** for**4**and **9** are 10 and 8.5 l mol^{-1}, respectively. All the above results are taken as evidence for the existence of octahedral geometry around the Co(II) ion**[31].**

The electronic spectra of the two green Ni(II) complexes (**3**and**10**) in DMSO, [Ni$\mathbf{L^1}_2Cl_2$].$4H_2O$ (**3**) and[Ni$\mathbf{L^2}_2Cl_2$].$3H_2O$ (**10**), shows three bands for each. The first complex (**3**) shows three bands at 9900, 15152 and 24390 cm^{-1} in DMSO assigned to $^3A_{2g} \rightarrow {}^3T_{2g}$ *(F),* $^3A_{2g} \rightarrow {}^3T_{1g}$ *(F)* and $^3A_{2g} \rightarrow {}^3T_{1g}$*(P)* transitions. Also, the second Ni^{2+} complex (**10**)

exhibits three bands in DMSO at 9990, 15846 and 24096 cm^{-1} attributed to $^3A_{2g} \rightarrow {}^3T_{2g}$ *(F)*, $^3A_{2g} \rightarrow {}^3T_{1g}$ *(F)* and $^3A_{2g} \rightarrow {}^3T_{1g}$*(P)* transitions in an octahedral geometry around the two Ni(II) ions [**30**]. The values of υ_1, B and β for the first Ni(II) ion were found to be 6467 cm^{-1}, 656 cm^{-1} and 0.63, while these values for complex (**10**) were found to be 9804 cm^{-1}, 702 cm^{-1} and 0.67, respectively, for the second Ni(II) ion. Also, the values of magnetic moments for the two complexes (**3** and **10**) are 2.90 and 3.24 BM, respectively. The results of electronic spectra and magnetic moments are taken as evidence for the existence of octahedral geometry around the Ni(II) ion **[31].**The electronic spectra of the two pale green Cu(II) complexes (**5** and**8**) in DMSO, [Cu$\mathbf{L^1}$$Cl_2$].$2H_2O$ (**5**) and [Cu$\mathbf{L^1_2}$$Cl_2$].$4H_2O$ (**8**), shows bands for each. The first Cu(II) complex show a band at 14925 cm^{-1} for the former Cu(II) complex **(5)** while a band centered at 15152 cm^{-1} for complex (**8**). These bands are attributed to $^2E_g \rightarrow {}^2T_{2g}$ transition in a distorted-octahedral geometry around the Cu(II) ion **[32]**. The values of magnetic moments of the two Cu(II) complexes are found to be 1.80 and 1.95 BM, respectively. Meanwhile, the electronic spectra of the two green Cr(III) complexes, [Cr$\mathbf{L^1}$$Cl_3$.$H_2O$].$3H_2O$ (**7)** and[Cr$\mathbf{L^2}$$Cl_3$.$H_2O$].$6H_2O$ (**13**), in DMSO shows two bands for each chelate. Complex (**7**) shows two bands at 20080 and 14970 cm^{-1} in DMSO assignable to $^4A_{1g} \rightarrow {}^4T_{2g}$ *(F)*and$^4A_{1g} \rightarrow {}^4T_{1g}$ *(F)* transitions. Also, the second Cr(III) complex (**13**) exhibits two bands in DMSO at 20833 and 14793 cm^{-1} assignable to $^4A_{1g} \rightarrow {}^4T_{2g}$ *(F)*and$^4A_{1g} \rightarrow {}^4T_{1g}$ *(F)* transitions in an octahedral geometry around the two Cr(III) ions [**30**]. Also, the values of magnetic moments for the two complexes (**7** and **13**) are found to be 3.87 and 3.95 BM, respectively. All the above results are taken as evidence for the existence of octahedral geometry around the Cr(III) ion**[31]**.

Finally, the electronic spectra of the two white Mn(II) complexes, [Mn$\mathbf{L^1_2}$$Cl_2$]$_2$.$16H_2O$ (**6)** and [Mn$\mathbf{L^2}$$Cl_2$]$_2$.$12H_2O$ (**14**), in DMSO shows four weak bands at 23,256-22727, 20,534-19939, 15,837-15,015 and 13,158-12,723 cm^{-1} attributed to$^6A_{1g} \rightarrow {}^4T_{2g}$ *(D)*, $^6A_{1g} \rightarrow {}^4A_{1g}$, $^6A_{1g} \rightarrow {}^4T_{2g}$ *(G)* and $^6A_{1g} \rightarrow {}^4T_{2g}$ transitions, respectively, which lie in the same range as reported for high-spin octahedral coordinated Mn(II) ion **[26].**The magnetic moments of the two complexes (**6** and **14**) are 5.84 and 6.14 BM, respectively. These values are taken as additional evidence for octahedral geometry around the Mn(II) ion.

3.5. Molecular modeling and DFT calculation studies

Molecular modeling study has been carried out to obtain insight into the structures of metal chelates. In addition a computational estimation has been performed to understand the mode of bonding in the chelates under investigation, theoretically using $DMOL^3$ program in materials studio package and Gaussian 09 program by density functional theory (DFT). The most significant orbitals in a molecule are the frontier molecular orbitals, HOMO and LUMO. The HOMO energy describes the electron donating ability, while LUMO energy describes the ability of electron acceptance for the compound. The HOMO helps to describe the chemical reactivity and kinetic stability of the molecule. In addition, it is a critical parameter to determine molecular electrical transport properties. It is very easy for electrons to be transferred from the ground to the excited state with such a small energy gap. So a molecule with small energy gap is characterized with a high chemical reactivity, low chemical stability and called as soft molecule. The energy gap (ΔE) of HOMO and

LUMO for both L^1 and $L^2$are shown in**Figs. 9 and 10**.

The energies of frontier molecular orbitals (E_{HOMO}, E_{LUMO} and band gap energy) result from DFT calculations obtained suggests about reactivity, molecular stability and site selectivity in addition to the donating ability. On using Koopman's theorem for closed shell components as electronegativity (χ), chemical potential (μ), global hardness (η), global softness (S) and global electrophilicity index (ω) **[33–35]** are computed using equations (**1–6**) listed in **Table 2**, HOMO and LUMO orbitals of Co(II)-$L^1$and Cr(III)-L^1 complexes are shown in **Figs. 11 and 12**. The donating ability of molecule can predict over the HOMO energy value where high energy values meaning tendency of donating electrons. The LUMO-HOMO energy gap concerning to stability in addition to hardness (η) and softness (S) related to reactivity where high E_{Gap} meaning high stability and smaller hardness less reactive molecule. The calculations of the values of the energy gap (ΔE) are 2.923 and 2.783 eV forL^1 and L^2**,** respectively, suggesting that $L^1$is less reactive than L^2. Accordingly, the stability of L^1 is more than L^2 and hence the softness of the former is better than the latter. The smaller values of hardness imply higher reactivity, which means that a molecule with a small LUMO – HOMO gap is more reactive and is a softer molecule. The soft molecules undergo changes in electron density more easily and are more reactive than hard molecules. The hardness value for complex is near or lowers than the ligand and hence its reactivity increases. All the computational calculations have been performed with Gaussian 09 program using Density Functional Theory (DFT) withBecke's three-parameter exchange and Lee-Yang-Parr correlation functional (B3LYP) with a combination of 6-311G++ (d, p) basis set for ligand.

Frontier molecular orbital analysis

$$\chi = -\frac{1}{2}\left(E_{HOMO} + E_{LUMO}\right) \quad (1)$$

$$\mu = -\chi = \quad (2)$$

$$\eta = \frac{1}{2}\left(E_{LUMO} - E_{HOMO}\right) \quad (3)$$

$$S = \frac{1}{2}\eta \quad (4)$$

$$\omega = \frac{\mu^2}{2\eta} \quad (5)$$

The inverse value of the global hardness bestowed the softness (σ) as follow:

$$\sigma = \frac{1}{\eta} \quad (6)$$

The results of frontier molecular orbital analysis for all complexes are shown in **Table 2**

3.6. Biological activity

3.6.1. Antibacterial and antifungal activity

The results of antibacterial activity (fungi; *Aspergillus flavus* and *Candida albicans*) for the two ligands ($L^1$and L^2**)** show that L^2 is better than L^1as shown in **Table 3**. In case of Gram-positive bacteria,(*Staphylococcus aureus*)the outcomes indicate that L^2 is better than L^1while in case of *Bacillus subtilis* (Gram +ive) L^1 gives better results than L^2

The findings ofGram-negatvie bacteria (*Escherichia coli* and *Proteus vulgaris*)illustrate that L^1 gives better results than L^2 and control. The results of antibacterial activity (fungi;*Candida albicans* and Gram-positive bacteria; *Bacillus subtilis*) against four chelates (Cu-L^1, Co-L^1, Cr-$L^1$and Mn-L^1)show that Co-L^1 gives better than the other chelates. In case of Gram-negatvie bacteria (*Proteus vulgaris*)the outcomes indicate that Cu-L^1 gives better than the other chelates as shown in **Table 4.**

.

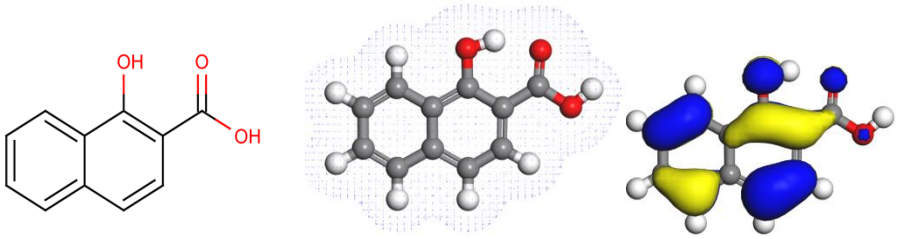

Fig. 1. Structure of*1*- hydroxy-*2*-naphthoic acid **(L[1])**

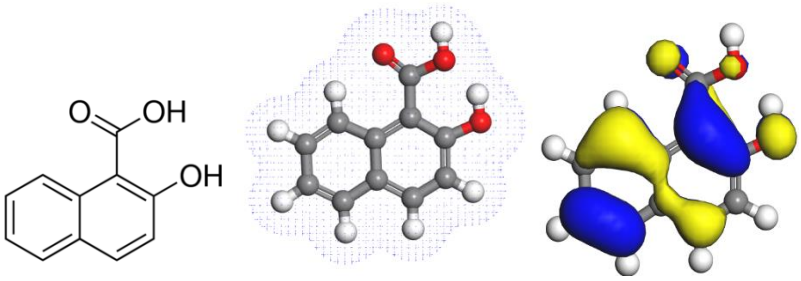

Fig. 2. Structure of *2*-hydroxy-*1*-naphthoic acid(**L[2]**)

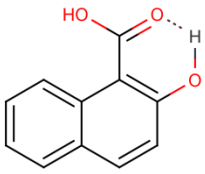

Fig. 3. Hydrogen bond in **L[2]**

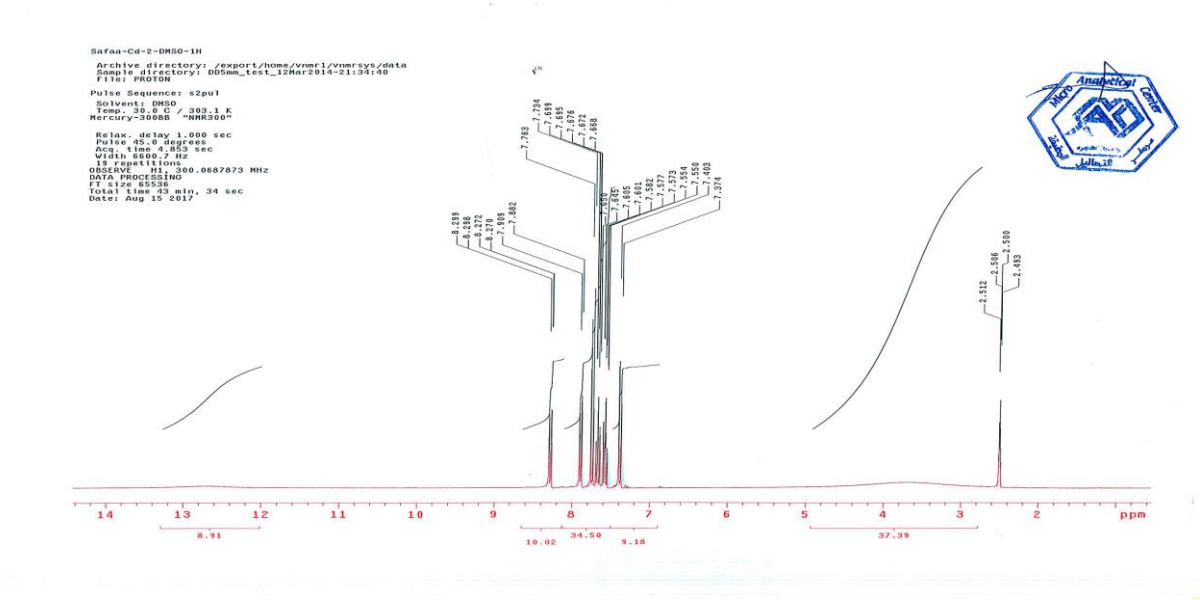

Fig. 4. ^{1}H-NMR spectrum of [Hg$\mathbf{L}^{2}$$Cl_2$].2$H_2O$ in d_6-DMSO

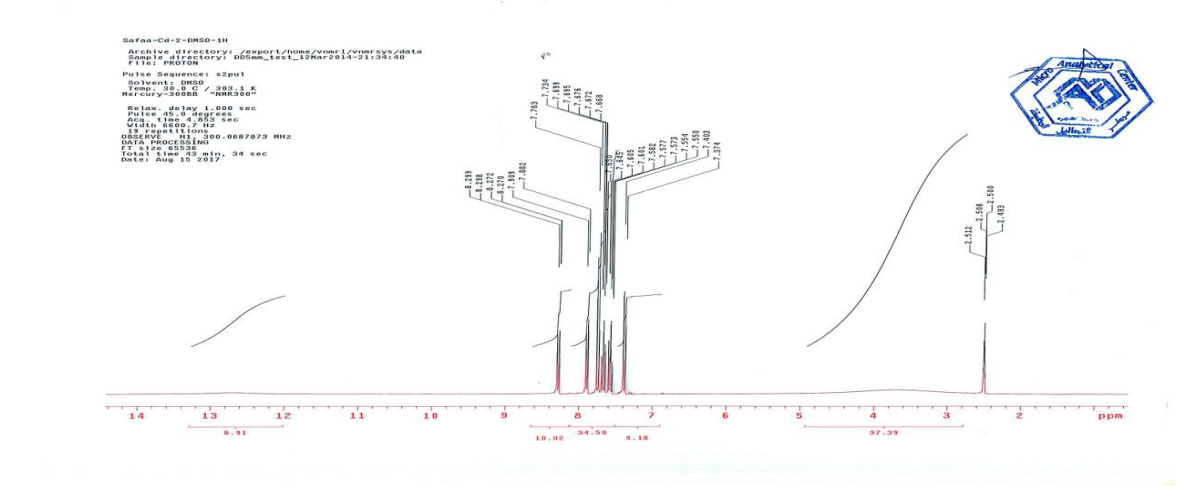

Fig. 5. ^{1}H-NMR spectrum of [Cd$\mathbf{L}_2{}^{2}$$Cl_2$].3$H_2O$ in d_6-DMSO

Fig. 6. ^{1}H-NMR spectrum of [Cd$\mathbf{L}_2^2$Cl$_2$].3H$_2$O in d$_6$-DMSO

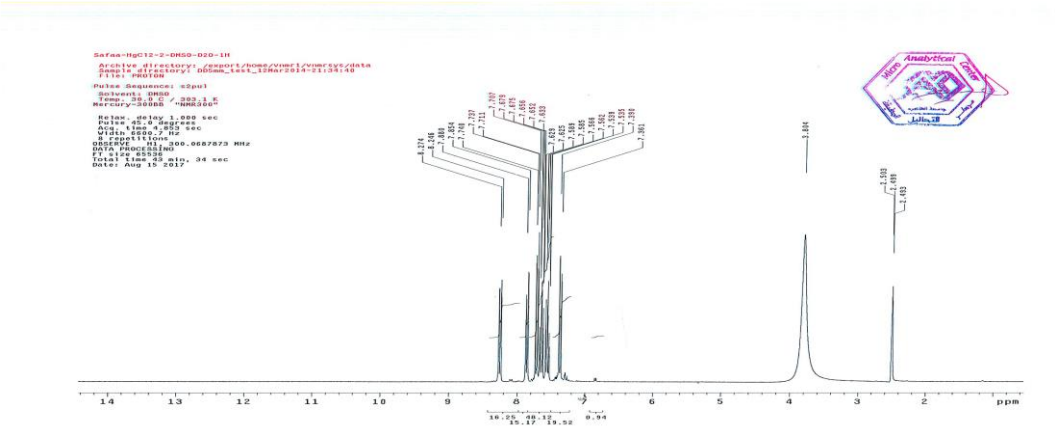

Fig. 7. ^{1}H-NMR spectrum of [Hg$\mathbf{L}^2$Cl$_2$].2H$_2$O d$_6$-DMSO+D$_2$O

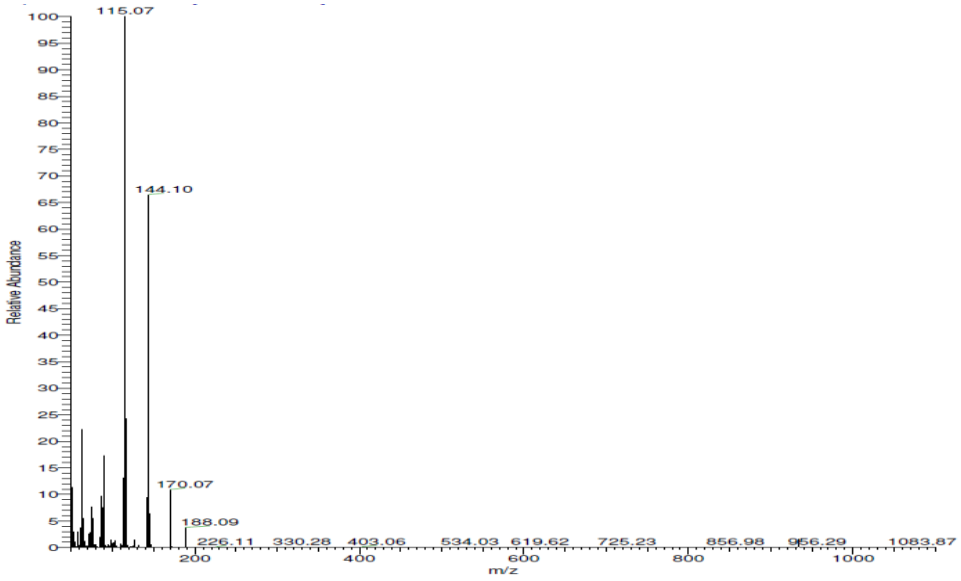

Fig. 8. Mass spectrum of [Mn($\mathbf{L^2}$)Cl_2].12H_2O.

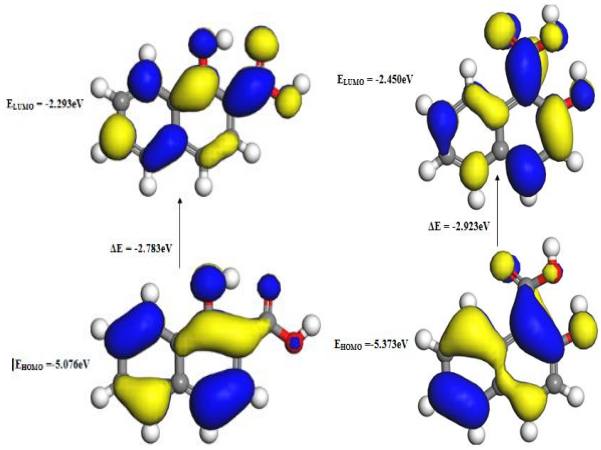

Fig. 9.HOMO-LUMO of $\mathbf{L^1}$**Fig. 10.**HOMO-LUMO of $\mathbf{L^2}$

Table 1. Elemental analyses of the solid chelates and some physical data.

No.	Chemical structure	MP (°C)	ύ (cm)	A^*_m DMSO	$\mu_{eff.}$, BM	% Found (Calcd.)			
						C	**H**	**M**	**Cl**
1	[Hg**L**^{1}$Cl_2(H_2O)_2$]; 495.713	166	35361, 33898, 30581	9.0	Diam	26.2 (26.7)	1.6 (2.4)	- -	14.1 (14.3)
2	[Cd**L**$^1_2$$Cl_2$].$H_2O$; 577.702	170	34843, 33138, 29674	3.0	Diam	45.5 (45.7)	2.8 (3.1)	19.3 (19.5)	11.9 (12.3)
3	[Ni**L**$^1_2$$Cl_2$].$4H_2O$; 578.05	150	34364, 24390, 15152, 9900	6.0	2.9	46.5 (45.7)	5.1 (4.2)	11.9 (10.2)	12.0 (12.2)
4	[Co**L**^{1}$Cl_2(H_2O)_2$]; 354.053	150	30303, 20833, 15624, 19833	7.0	5.47	37.3 (37.3)	3.6 (3.4)	16.1 (16.6)	19.7 (20.0)
5	[Cu**L**^{1}Cl_2].$2H_2O$; 358.663	189	30225, 20733, 14925	3.7	1.80	37.0 (36.8)	3.5 (3.4)	17.3 (17.7)	19.2 (19.8)
6	[Mn**L**$^1_2$$Cl_2$]$_2$.$16H_2O$; 1292.688	280	36490, 34965, 29955, 5067, 12767	3.8	5.84	41.1 (40.9)	4.4 (5.0)	8.0 (8.5)	10.5 (11.))
7	[Cr**L**^{1}Cl_3.H_2O].$3H_2O$; 418.608	230	29674, 20080, 14970,	2.0	3.87	31.7 (31.6)	3.7 (3.9)	12.-0 (12.4)	24.8 (25.4)
8	[Cu**L**$^1_2$$Cl_2$].$4H_2O$; 582.88	240	29762, 15152	7.0	1.95	46.0 (45.3)	2.8 (3.5)	10.6 (10.9)	11.8 (12.2)
9	[Co**L**$^2_2$$Cl_2$]$_2$.$6H_2O$; 1120.508	200	20921, 19608, 15873	5.0	5.1	46.8 (47.2)	2.9 (4.0)	38.5 (10.5)	12.1 (12.7)
10	[Ni**L**$^2_2$$Cl_2$].$3H_2O$; 560.054	210	24096, 15846, 9900	7..0	3.14	46.9 (47.2)	3.4 (4.0)	9.9 (10.5)	12.2 (12.7)
11	[Cd**L**$^2_2$$Cl_2$].$3H_2O$; 613.734	202	34482, 33113, 29240	9.0	Diam.	43.5 (43.1)	3.2 (3.6)	17.6 (18.3)	11.0 (11.6)
12	[Hg**L**^{2}Cl_2].$2H_2O$; 495.713	196	36101,32787, 29674, 28169	3.0	Diam.	26.8 (26.7)	1.6 (2.4)	- -	14.0 (14.3)
13	[Cr**L**^{2}Cl_3.H_2O].$6H_2O$; 472.656	208	29326, 20833, 14493	5.0	3.95	27.3 (28,0)	4.9 (4.7)	9.8 (11.0)	22.3 (22.5)
14	[Mn**L**^{2}Cl_2]$_2$.$12H_2O$; 1060.446	130	34483, 33003, 29326, 20921	3.0	6.14	24.1 (24.9)	5.3 (6.1)	9.7 (10.4)	12.8 (13.4)

Table 2. Calculated total energy, E_{HOMO}, E_{LUMO}, gap energy (E_L - E_H), hardness (η), softness (σ) and dipole moment (μ) for the isolated chelates.

Calculated total energy, E_H, E_L, gap energy (E_L – E_H), chemical potential (μ), electronegativity (χ), global hardness (η), global softness (S) and global electrophilicity (ω) for isolated complexes

No.	**Dipole moment (Debye)**	**E_H (eV)**	**E_L (eV)**	**E_{Gap}(eV)**	**χ (eV)**	**μ (eV)**	**η (eV)**	**S (eV)**	**ω (eV)**	**σ (eV)**
CdL^1	13.032	-5.586	-1.106	4.48	3.346	-3.346	2.42	1.21	2.3131	0.41322
CrL^1	9.476	-5.434	-4.023	1.411	4.7258	-4.7258	0.7055	0.35275	15.827	1.4174
MnL^1	2.295	-5.441	-2.582	2.859	8.023	-8.023	1.4295	0.71475	22.514	0.69954
NiL^1	1.800	-6.031	-5.639	0.392	5.835	-5.835	0.196	0.098	86.8551	5.1020
CoL^1	2.891	-6.199	-5.695	0.504	5.947	-5.947	0.252	0.126	70.172	3.9682
CuL^1	4.811	-4.406	-4.791	-0.731	4.5985	-4.5985	0.3655	0.18275	28.927	2.7359
HgL^1	13.410	-5.505	-1.603	3.902	3.554	-3.554	1.951	0.9755	3.2370	0.51255
CdL^2	18.80	-8.099	-5.808	2.291	6.9535	-6.9535	1.1455	0.57275	21.1048	0.87298
HgL^2	9.1512	-6.335	-5.621	0.714	5.978	-5.978	0.357	0.1785	50.051	2.8011
MnL^2	16.188	-6.476	-5.976	0.5	6.226	-6.226	0.25	0.125	77.526	4.00
NiL^2	6.5368	-5.893	-5.855	0.038	5.874	-5.874	0.019	0.0095	90.99	5.23631

Co(II)-L^1 complex:

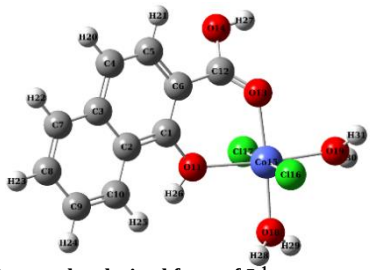

Co complex derived from of L^1

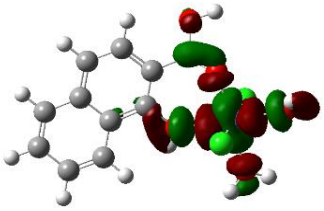

HOMO of Co complex derived from L^1

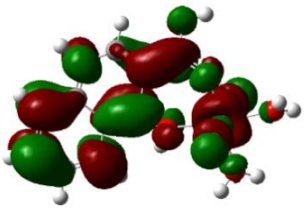

LUMO of Co complex derived from L^1

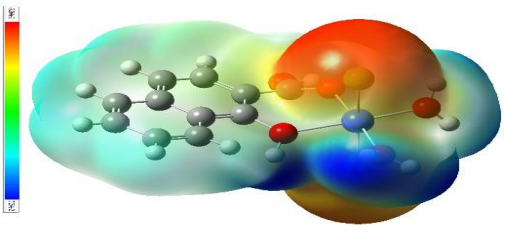

ESP of Co complex derived from L^1

Fig. 11. HOMO and LUMO for Co(II)-L^1 complex

Cr(III) complex-L[1]:

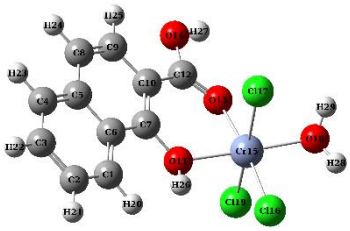

Cr complex derived from L[1]

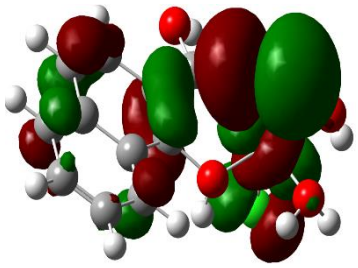

Homo of Cr complex derived from

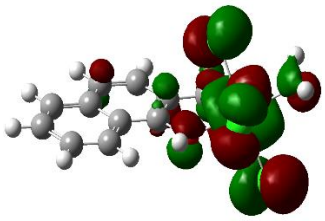

Homo of Cr complex derived from L[1]

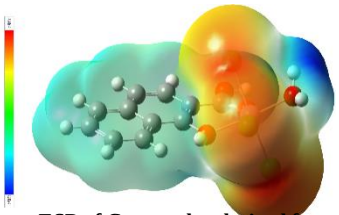

ESP of Cr complex derived from L[1]

Fig. 12. HOMO and LUMO for Cr(III)-L[1] complex

Table 3. Antimicrobial [fungi, (Gram +ive and Gram +ive)] results of **L[1]** and **L[2].**

	L[1]	**L[2]**	Control
Fungi			*Ketoconazole*
Aspergillus flavus (RCMB 002002)	25	29	16
Candida albicans RCMB 005003 (1) ATCC 10231	12	13	20
Gram-positive bacteria			*Gentamycin*
Staphylococcus aureus (RCMB010010)	13	14	24
Bacillus subtilis RCMB 015 (1)NRRL B-543	14	12	26
Gram-negatvie bacteria			*Gentamycin*
Escherichia coli(RCMB 010052)ATCC 25955	15	13	30
Proteus vulgaris RCMB 004 (1) ATCC 13315	14	12	25

Table 4. Antimicrobial results of the synthesized *1*-hydroxy-*2*-naphthoic (**L[1]**) acid chelates.

Sample code / **Tested microorganisms**	**Cu-L[1]**	**Co-L[1]**	**Cr-L[1]**	**Mn-L[1]**	**Control**
FUNGI					Ketoconazole
Candida albicans **RCMB 005003 (1) ATCC 10231**	11	14	12	10	20
Gram Positive Bacteria:					*Gentamycin*
Bacillus subtilis RCMB 015 (1)NRRL B-543	20	22	17	15	26
Gram Negatvie Bacteria:					*Gentamycin*
Proteus vulgaris **RCMB 004 (1) ATCC 13315**	22	19	15	14	25

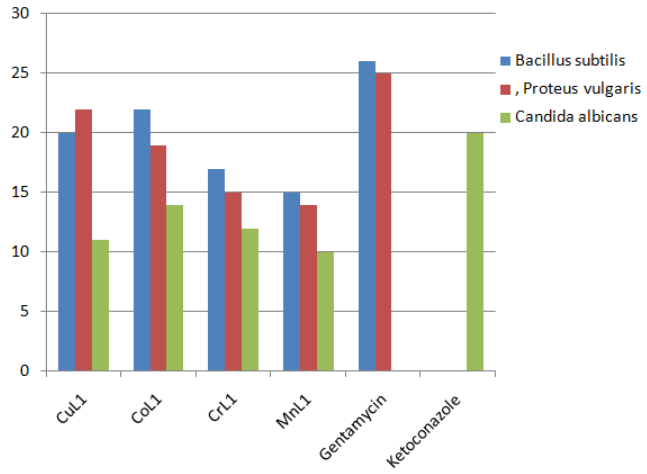

Figure 14. Antimicrobial results of the synthesized *1*-hydroxy-*2*-naphthoic acid chelates

Table 5. Breast results of **L[1]**.

Sample	Breast cancer	Hepatocellular cancer
1-hydroxy-2-naphthoic acid (**L[1]**)	47.3	24.2

Table 6. Inhibition of cell proliferation ($IC_{50\mu g}$ sample/l) for the chelates.

Chelates	Breast cancer
Co + L^1	31
Mn + L^1	45.3
Cr + L^1	90.7
Cu + L^1	14

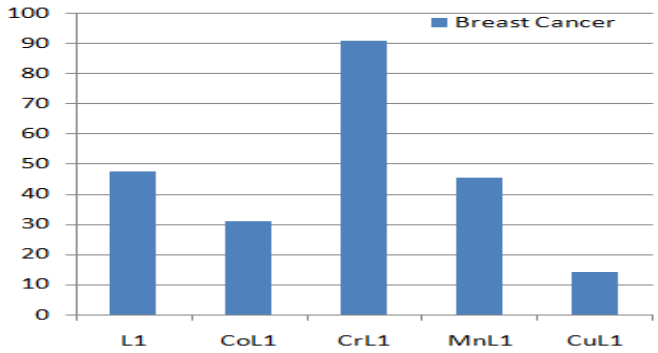

Figure 15. Scavenging capacities (IC_{50}) of **L^1**and some metal chelates toward mammary gland breast cancer (MCF-7).

3.6.2. Antitumor activity using in vitro cytotoxic activities

The scavenging capacities (IC_{50}) of **L^1**and some metal chelates toward mammary gland breast cancer (MCF-7) are shown in **Tables 5, 6** and depicted in **Figure 15.** From the graph plotted between cell viability (percentage) and concentration the scavenging capacities (IC50) values were calculated in **Figure 15.** 5-Fluorouracil has been also assayed as standard. Vitro cytotoxicity tests were conducted utilizing **L^1** and the four prepared compounds (**Co + L^1, Mn + L^1,Cr + L^1**and **Cu + L^1**) against breast cancer. The data is depicted in **Table 6** showing that:

i.Cu + L^1 has IC50 (14 µg/ml) in comparison to **Co + L^1** (31 µg/ml), **Mn + L^1** (45.3 µg/ml) and **Cr + L^1** (90.7 µg/ml) indicating that Cu chelate is strong cytotoxic against breast cancer cell line without causing significant damage to the normal cells.

ii. The value of IC50 in case breast cancer of Cu complex is 14 suggesting that the Cu chelate has a strong cytotoxic activity. The increased activity of the metal chelates can be explained on the basis of the overtone concept and chelation theory **[36].** Where, the overlap of the ligand orbital and the partial sharing of the positive charge of the metal ion with donor groups reduce the polarity of the metal ion largely and so increase the delocalization of electrons over the completely chelate ring and consequently

optimize the lipophilicity of the chelate. Thus enhances the penetration of the chelate into the lipid membrane and blocks the metal binding sites on the enzymes of the microorganism .

4. CONCLUSIONS

Fourteen new binary chelates were synthesized from the ligands ($\mathbf{L^1}$ and $\mathbf{L^2}$) under investigation with some metal chlorides by tribochemical reaction in the solid state. The isolated chelates are characterized by chemical, spectral (IR, UV-Visible, ^{1}H-NMR, mass) and magnetic methods. Bidenate behavior of the two ligands ***via*** the phenolic OH and the CO (carboxylate) groups without displacement of a hydrogen atom from the carboxylate and/or the phenolic groups towards the metal ions. Octahedral geometries for the isolated chelates were suggested by spectral and magnetic data and confirmed by material studio program.DFT calculations suggest the most suitable geometry as well as the stability of the complexes. The energy gap, chemical reactivity, binding energies and dipole moments for all compounds were evaluated using density functional theory and molecular electrostatic potential for $\mathbf{L^1}$and $\mathbf{L^2}$.The mass spectra of some metal chelates illustrate that these compounds are existed as dimer. Some chelates were tested against fungi and bacteria. Also, the ligands and some of their complexes were tested as anticancer using **MCF-7** cells (human breast cancer cell line) and **HepG-2** cells (human Hepatocellular carcinoma)

REFERENCES

1. Kozlowski, H., Bal, W., Dyba, M., Kowalil-Jankowska, T., Specific structure-stability relations in metallopeptides. Coord. Chem. Rev., 184, 319-346 (1999).

2. Farrell, N., Transition metal complexes as drugs and chemotherapeutic agents. Kluwer, Dordrecht (1989).

3. Shoukry E.M., Khairy E.M., A.A. Shoukry A.A., Shoukry M.M., Equilibrium investigation of complex formation reactions of the trigonal-bipyramidal complex $[Cu(Tren)(OH_2)]^{2+}$ with amino acid, peptide or DNA constituent, Egypt. J. Chem., 45 (6), 1127 (2002).

4. Aml G. A., Shoukry E.M., Mostafa M.M.,Equilibrium studies of binary and ternary complexes involving 2-hydroxy-1-naphthoic acid and amino acids in dioxane–water mixture, Egypt. J. Chem., 64, (2), 623 -630(2021).

5. Dogan, H.N., Rollas, S., Erdeniz, H., Synthesis, structure elucidation and antimicrobial activity of some *3*-hydroxy-*2*-naphthoic acid hydrazide derivatives, Farmaco, 53, 462-467 (1998).

6. Mostafa, M.M., Gomma, E.A.H., Mostafa M.A., El-Dossouki, F.I., Spectroscopic studies of complex compounds derived from the tribochemistry reactions of KBr and HgX_2 (Cl, Br, I, CN) with crown ethers (DC18C6 and DB18C6), Spectrochim. Acta, **A**, 55, 2869-2875 (1999).

7. Mostafa, M.M., Gomma, E.A.H., Mostafa, M.A., El-Dossouki, F.I., Complexes of some crown ethers with Hg(II) chloride, bromide, iodide and cyanide Synth. React. Inorg. Met Org. Chem., 30 (1), 157-174 (2000).

8. Mostafa, M.M., Abdel-Rhman, M.H.,Spectroscopic studies of some novel Cu^{I} and Cu^{II} complexes derived from the tribochemistry reactions of KBr, KI and CaI_2 with Cu^{II}–Girard's T complex $[Cu(GT)Cl_2(H_2O)_2(EtOH)]Cl\cdot H_2O$, Spectrochim. Acta, A, 2341-2349 (2000).

9. Mostafa, M.M., El-Shazly, R.M., Rakha, T.H., Abdel-Rhman, M.H., The dangers of using KBr, KI and CaI_2 as mulling agents during the preparation of infrared discs of complexes, Trans.Met. Chem., 27 (3), 337-340 (2002).

10. Mostafa, M.M., Abdel-Rhman, M.H., the spectroscopic studies of some novel Ru(III) complexes derived from the tribochemical reactions of KBr and Ki with Ru(III)-girard's T complex, Intern. J. Chem., 14 (1), 17 (2004).

11. Al-Radadi, N.S., Al-Ashqar, S.M., Synthesis and characterization of some new binary and ternary

Cu^{II} complexes. Synth. React. Inorg. Met-Org. Nano Met. Chem., 41, 1-8 (2011).

12. Al-AshqarS.M., Comparative studies of new complexes synthesized by chemical and tribochemical reactions derived from malonic acid dihydrazide (L; MAD) with Cu^{2+} and Co^{2+} salts, OJIC, 8, 28-42 (2018).

13. Al-Ashqar, S.M., Mostafa, M.M., Synthesis and characterization of Cu^{II} and Co^{II} complexes derived from 2,4,6-tri-(2-pyridyl)-1,3,5-triazine (TPT) by chemical and tribochemical reactions, J. Coord. Chem., 63, 721-729 (2010).

14. Al-Ashqar, S.M., Mostafa M.M., Synthesis of some novel Co^{II} and Co^{III} complexes by tribochemical reactions using KI with some derivatives of thiosemicarbazide complexes derived from Girard's T and P, Spectrochim Acta, 171(4), 1321-6 (2008).

15. Badawi, A.M., Shoukry. E.M., Amine, M.F., Mohamed, M.A., Moustafa, A.G., Mostafa, M.M., Comparative, synthesis and characterization studies of some metal complexes derived from L-lysine.HCl and L-lysine.2HCl by tribochemical reactions (part 2). Inorg. Chem., J. Indian,10(2), 66-72 (2015).

16. Moustafa, A.G., Badawi, A.M., Shoukry. E.M., Amine, M.F., Mostafa, M.M., Comparative, synthesis and characterization studies of some metal complexes derived from L-lysine.HCl and L-lysine.2HCl by tribochemical reactions. 10(4), 135-141 (2015). 17. Al-Ashqar, S.M., Comparative studies between chemical and tribochemical reactions of some metal complexes derived from N-(O-hydoxyphenyl)-N'-phenylthiourea (L), Open J. Inorg. Chem., 6, 195-204 (2016)

18. Al-Ashqar, S.M., Comparative studies of new complexes synthesized by chemical and tribochemical reactions derived from malonic acid dihydrazide (L; MAD) with Cu^{2+} and Co^{2+} salts, Open J. Inorg. Chem., 8, 28-42 (2018).

19. Shoukry, E.M., Amin, M.F., Badawi, A.M.,Mohamed, M.A., Ahmed, A.G., Equilibrium studies of complex formation reactions of $[Pd(SMC)(H_2O)_2]^+$ with amino acids, peptides or DNA constituents. Egypt. J. Chem.,58(1), 71-83,(2015).

20. Shoukry, E.M., Hosny, N.G., Amin, M.F., Mohamed, E.F., Complex formation equilibria of ternary complexes of Cu(II) involving pyridine-2-carboxylic acid and various biologically relevant ligands Int., J. Curr. Res. Chem. Pharm. Sci. 3(10): 32-43 (2016).

21. Shoukry, E.M., Hosny, N.G., Amin, M.F., Mohamed, E.F., Mixed ligand complex formation reactions and equilibrium studies of diaqua(N-methylethylenediamine) palladium(II) with various biologically relevant ligands, J. Chem. Bio. Phys. Sci. (A), 6, 1308-1328 (2016).

22. Vogel, A.I., Text book of Quantitative Chemical Analysis, 5th Edition, Chapter 15, p. 555, Longman, UK (1989).

23. Mosmam, T., J. Immunol. Methods, Rapid colorimetric assay for cellular growth and survival applications to proliferation and cytotoxicity assay, 65, 55-63 (1983).

24. Mauceri, H.J., Hanna, N.N., Beckett, M.A., Gorski, D.H., Staba, M.J., Stellato, KA., Bigelow, K., Heimann, R., Gately, S., Dhanabal, M., Soff, G.A., Sukhatme, V.P., Kufe, D.W., Weichselbaum, R.R., Combined effects of angiostatin and ionizing radiation in antitumour therapy, Nature 394, 287-291 (1998).

25. Wilson, A.P., Cytotoxicity and viability assays in animal cell culture: A practical approach, 3rd Edn., (Edit, J. R.W. Masters), Oxford University Press, 175-219, (2000).

26. Rahman, A.U., Choudhary, M.I., Thomsen, W.J., Bioassay techniques for drug development, CRC Press, Taylor& Francis Group, Amsterdam (2001).

27. Sumrra, S.H., Chohan, Z.H., In vitro antibacterial, antifungal and cytotoxic activities of some triazole Schiff bases and their oxovanadium(IV) complexes, J. Enz. Inhib. Med. Chem., 28, 1291-1299 (2013).

28. Senti, F., Harker, D., The crystal structure of rhombohedral acetamide, J. Am. Chem. Soc., 62, 2008-2019 (1940).

29. Ferraro, J.R., Low frequency vibration of inorganic and coordination compounds, Plenum Press, New York, (1971).

30. Lever, A.B.P. Inorganic electronic spectroscopy; Elsevier,Amsterdam, (1984).

31. Kato, M., Jonassen, H.G., Fanning, J.C., Copper(II) complexes with subnormal magnetic moments, Chem. Rev., 64, 99-128 (1964).

32. Maztesanz, A.I., Perez, J.M., Navarro, P., Moreno, J.M., Colacio, E.,Souza, P., Synthesis and characterization of novel palladium(II) complexes of bis(thiosemicarbazone) structure, cytotoxic activity and DNA binding of Pd(II)-benzyl bis(thiosemicarbazonate), J. Inorg. Biochem., 76, 29-37 (1999).

33. Thanikaivelan, P., Subramanian, V., Rao, J.R., Nair, B.U., Application of quantum chemical descriptor in quantitative structure activity and structure property relationship Chem. Phys. Lett., 323, 59-70 (2000).

34. Mlahi, M.R., Negm, A., Azhari, S.J., Mostafa, M.M., Synthesis, characterization, molecular modelling and biological activity of 2-(pyridin-1-ium-1-yl) acetate and its Cu^{2+}, Pt^{4+}, Pd^{2+}, Au^{3+} and Nd^{3+} complexes, Appl. Organomet. Chem., 28, 712-719 (2014).

35. Mostafa A.M., Shoukry E.M., Shehata M.R., Mohamed E.F., Kinetic mechanism and DFT calculations on base hydrolysis of α- amino acid esters catalyzed by$[Pd(TMPDA)\ (H_2O)_2]^{2+}$, Egypt. J. Chem, 64(2), 903-912(2021).

36. Hassan, E.A., Nawar, N., Mostafa, M.M., Comparative studies of some novel Cu^{2+} and Fe^{3+}chelates derived from tricine (L1) by single crystal X-ray, spectroscopic and biological data: applications to investigate antitumor activity. Appl.Organometallic. Chem. 2019; 33: e5096. https://doi.org/10.1002/aoc.5096.